

Journal of Materials Chemistry B

Accepted Manuscript



This is an *Accepted Manuscript*, which has been through the Royal Society of Chemistry peer review process and has been accepted for publication.

Accepted Manuscripts are published online shortly after acceptance, before technical editing, formatting and proof reading. Using this free service, authors can make their results available to the community, in citable form, before we publish the edited article. We will replace this *Accepted Manuscript* with the edited and formatted *Advance Article* as soon as it is available.

You can find more information about *Accepted Manuscripts* in the [Information for Authors](#).

Please note that technical editing may introduce minor changes to the text and/or graphics, which may alter content. The journal's standard [Terms & Conditions](#) and the [Ethical guidelines](#) still apply. In no event shall the Royal Society of Chemistry be held responsible for any errors or omissions in this *Accepted Manuscript* or any consequences arising from the use of any information it contains.

Prompt and Synergistic Antibacterial Activity of Silver Nanoparticle-Decorated Silica Hybrid Particles on Air Filtration

Cite this: DOI: 10.1039/x0xx00000x

Received 00th January 2012,
Accepted 00th January 2012

DOI: 10.1039/x0xx00000x

www.rsc.org/

Young-Seon Ko^a, Yun Haeng Joe^b, Mihwa Seo^a, Kipil Lim^a, Jung-ho Hwang^b, and Kyoungja Woo^{*a,c}

There is a significant need for materials that promptly exhibit antimicrobial activity upon contact. The large-scale fabrication of monodisperse silver nanoparticle (AgNP)-decorated silica (AgNP@SiO₂) hybrid particles, and their prompt and synergistic antibacterial activity against both Gram-negative bacteria *Escherichia coli* and Gram-positive bacteria *Staphylococcus epidermidis* on air filtration are presented. Monodisperse aminopropyl-functionalized silica colloids (406 nm) were used as a support material and were hybridized with AgNPs using seeding, sorting-out, and growing strategy of Ag seeds (1–2 nm) into ~30 nm AgNPs, successfully yielding 51 g of AgNP@SiO₂ hybrid particles. Medium filter samples (glass fiber material, 4 × 4 cm²) were coated with AgNP@SiO₂ particles and tested for antibacterial efficacy. SEM characterization of the bacterial morphology suggested prompt and synergistic antibacterial activity against both classes of bacteria. Additionally, antibacterial efficacies > 99.99% for both bacteria were obtained using a filter sample with a coating areal density of 1 × 10⁸ particles/cm². Solutions of AgNP@SiO₂ at 1.3% were stable even after 8 months. The hybrid particle AgNP@SiO₂ and the air filter system coated with the particles are expected to be useful for future green environment applications.

Introduction

Outbreaks of infectious diseases caused by airborne microorganisms present a significant threat worldwide. As a result, antimicrobial materials have attracted great attention. The development of a material that can promptly exhibit antimicrobial activity after coated on the appliances (*i.e.* air filters, air conditioners, and paint, *etc.*) is highly desired because the deposited microorganisms can survive and multiply when appropriate moisture and deposited nutrient dusts are present.^{1–5} The multiplied microorganisms as well as volatile organic compounds produced by the microbial metabolism can eventually be released into the air.^{2,3,6,7} This possibility highlights the need for a material which can promptly exhibit antimicrobial activity upon contact at its coated state on the medium. In addition to prompt antimicrobial activity, the coating material should also be amenable to large-scale fabrication with monodisperse size distribution for practical utilizations.

Silver and silver containing materials such as silver nanoparticles (AgNPs) and Ag⁺ ions are known to be potent antimicrobial agents.^{4–6,8–13} In particular, Ag⁺ ions in aqueous solution have shown great antimicrobial activity, and their antimicrobial mechanism has been studied widely.^{5,8} Ag⁺ ions interact with the proteins on the bacterial membrane and penetrate into the cell, where they interact with DNA and RNA. These interactions change the structure and function of target

molecules and eventually lead to cell death. Antimicrobial efficacy normally appears after treatment for 2 h to several days, depending on the Ag⁺ concentration. On the other hand, the antimicrobial activity of AgNPs has been debated. A clear-cut distinction between the antimicrobial activity of AgNP and that of Ag⁺ has been difficult because AgNPs are oxidized by oxygen and release Ag⁺ ions. Therefore, AgNPs and Ag⁺ ions always coexist in aerobic aqueous solutions.^{14–16} This issue was recently investigated using poly(ethylene glycol)-thiol-coated AgNPs in an anaerobic aqueous solution to prohibit the release of Ag⁺ ions.¹⁶ It was reported that the antibacterial activity of AgNPs in the anaerobic aqueous solution mainly comes from the previously oxidized and dissolved Ag⁺ ions and that the particle-specific antibacterial activity is negligible.¹⁶ Prior to this, Sondi et al. reported that AgNPs make pits on the membranes of Gram-negative bacteria (*Escherichia coli*) and lead to cell death in aerobic aqueous solutions.⁹ Supporting reports have indicated enhanced antibacterial effect under co-existence of AgNPs and dissolved Ag⁺ ions, rather than only Ag⁺ ions at constant concentrations.^{17–19} In particular, comparable antibacterial activities of AgNPs and the released Ag⁺ ions have been observed for AgNPs larger than ~15 nm,^{18,19} whereas the antibacterial activity is dominated by the released Ag⁺ ions for AgNPs smaller than ~10 nm.¹⁸ It is noteworthy that AgNPs^{9,17–19} which have shown enhanced antibacterial activity in addition to that of Ag⁺ ions have had a partially naked surface due to their labile ligands or their hybrid

structure. Unfortunately, fully naked AgNPs cannot exist as a colloidal solution due to their aggregation caused by high surface energy.

A silica hybrid colloid encapsulating a magnetite core and decorated with 30 nm-sized AgNPs ($\text{AgNP@SiO}_2/\text{Fe}_3\text{O}_4$)²⁰ and a magnetite-silica Janus nanorod decorated with 5 nm-sized AgNPs ($\text{AgNP@Fe}_3\text{O}_4\text{-SiO}_2$)²¹ have been reported as a magnetically collectable antimicrobial material in water. Both reports used the silica material as a biocompatible, water-dispersible, and physico-chemically stable inorganic support for the naked AgNPs. The former colloid exhibited immediate and synergistic antibacterial activity compared to the latter Janus nanorod, due to the large (30 nm vs. 5 nm) and many AgNPs in three-dimensional structure on a silica support.²⁰ However, hybridization of silica with magnetic material encumbers a synthesis process with an extra complexity, particularly for a large-scale fabrication. Moreover, magnetic property is not necessarily for a coating material which is applied on the appliances such as air filters and air conditioners. Thus, monodisperse silica hybrid particles decorated with AgNPs of ~30 nm may be a reliable candidate as a prompt antibacterial coating material.

Researchers have coated Ag^+ ion-containing materials and AgNPs or their carbon composites on glasses and air filters using various methods and have reported antibacterial efficacy by the colony count method (CCM) or by the disk diffusion method (DDM), which are generally used worldwide.^{4,5,13,22–26} The CCM is a method to count the bacterial colony number after spreading a specimen-treated bacterial solution on an agar plate and incubating for approximately 24 h. The DDM is based on the appearance of a belt-like inhibition zone surrounding the specimen after placing it on the nutrient agar in bacterial solution and incubating for approximately 24 h. Both methods evaluate antibacterial activity after incubation of aqueous bacterial solution with the Ag^+ - or AgNP-coated specimen. Fundamentally, these evaluation methods do not differentiate the antibacterial effect of Ag^+ ions from that of AgNPs which release Ag^+ ions into aerobic water. To the authors' knowledge, there has been no substantiated coating material showing a prompt antibacterial activity in air. Therefore, the material which can promptly show antibacterial activity in air at its coated state is in great need.

In this report, the large-scale (51 g) fabrication of monodisperse silica hybrid particles decorated with ~30 nm-sized AgNPs (AgNP@SiO_2), and their prompt and synergistic antibacterial activity against both Gram-negative bacteria *Escherichia coli* (*E. coli*) and Gram-positive bacteria *Staphylococcus epidermidis* (*S. epidermidis*) on air filtration are presented.

Experimental

Materials

Ethanol (Burdick & Jackson, 99.9+%), NH_4OH (Junsei, 28.0–30.0%), tetraethylorthosilicate (TEOS, Sigma Aldrich, 98%), 3-(aminopropyl)trimethoxysilane (APTMS, Sigma Aldrich, 97%), tetrakis(hydroxymethyl)phosphonium chloride (THPC, Sigma Aldrich, 80% solution in water), formaldehyde (Sigma Aldrich, 37% solution in 10–15% methanol), AgNO_3 (Sigma Aldrich, > 99.0%), NaOH (Showa, 93.0%), and HCl (Matsuno Chemicals Ltd., 35%) were used as purchased.

Characterization

The TEM images were recorded using a CM30 (Philips, 200 kV). The SEM images were recorded using a FEI XL30-ESEM or NOVA200 NOVA-SEM. All of the SEM samples were coated with Pd/Pt for 20 sec (HITACHI, E-1010 Ion Sputter). X-ray photoelectron spectroscopy (XPS) data were obtained with a PHI 5000 VersaProbe (Ulvac-PHI) using monochromatic Al $\text{K}\alpha$ radiation (1486.6 eV). For XPS sample preparation, one drop of the sample solution was placed on a silicon wafer and naturally dried. X-ray diffraction (XRD) patterns were measured by a Rigaku Dmax 2500 with Cu $\text{K}\alpha$ radiation ($\lambda = 1.5406 \text{ \AA}$). UV–Vis spectra were recorded using a Perkin Elmer Lambda 25 with a 1 cm-cell.

Fabrication of aminopropyl-functionalized silica sphere (APSiO_2)

The typical Stöber process²⁷ with appropriate modifications was applied to fabricate silica spheres. In a tailor-made 20 L reactor with a mechanical stirrer at ambient temperature (20–25 °C), 8 L of ethanol, 0.8 L of deionized water (DW), and 0.24 L of NH_4OH were stirred. 0.48 L of TEOS was then added and stirred for 5 h, yielding ~280 nm silica spheres. Consecutively, 0.8 L of DW followed by 0.48 L of TEOS was added and stirred for 5 h to grow silica spheres. This step was repeated once more, yielding ~400 nm silica spheres. For aminopropyl (AP)-functionalization, 9 mL of APTMS diluted in 30 mL of ethanol was added and stirred overnight. The resultant APSiO_2 was centrifuged, washed with 2 L of ethanol 6 times using centrifugation, and finally dispersed in 2.5 L of ethanol. This process yielded a stock solution of 16.94% by weight/volume (16.94 g in 100 mL) with a diameter of $406 \pm 17 \text{ nm}$ (average \pm standard deviation), as measured by TEM analysis.

Fabrication of AgNP@SiO_2

Two hundred mL of 16.94% APSiO_2 stock solution was centrifuged and dispersed in 100 mL of DW. By adding 400 mL of 0.1 M HCl, the solution was adjusted to pH~4 and stirred for 15 h to achieve a homogeneous dispersion. To prepare Ag seeds with 1–2 nm size at ambient temperature, 720 mL of DW and 80 mL of 0.1 M NaOH solution were mixed in a 1 L Pyrex glass bottle with a cap. To this solution, 0.34 mL (1.9 mmol) of THPC was added as a reducing agent. After stirring for 2 min, 32 mL (1.9 mmol) of 1% AgNO_3 solution was poured and the solution was stirred for 15 min. Five sets of the Ag seed solution were prepared simultaneously and combined in a 5 L Pyrex glass bottle with a cap. The APSiO_2 solution prepared above was then poured into the 5 L bottle containing the Ag seeds and gently swirled every 30 min for Ag seeding onto the APSiO_2 . After 2 h, the solution was centrifuged and the $\text{Ag}_{\text{seed}}\text{@SiO}_2$ solid was dispersed in 500 mL of DW. Meanwhile, in a tailor-made 50 L reactor (Fig. S1) equipped with a chiller jacket for temperature control ($12 \pm 1 \text{ }^\circ\text{C}$) and mechanical stirrer, 35 L of distilled water and 21 g of AgNO_3 were combined and stirred. When 21 mL of NH_4OH was added and stirred, the suspension became transparent. This implicates a formation of $[\text{Ag}(\text{NH}_3)_2]^+$ complex, which is amenable to controlled reduction to Ag due to its lower standard reduction potential (+0.38 V) than that (+0.80 V) of Ag^+ .¹⁹ Then, the $\text{Ag}_{\text{seed}}\text{@SiO}_2$ solution was poured into the reactor and stirred for 30 min to sort out the relatively larger seeds. The larger seeds sorted out are coalesced together and later, removed by centrifugation. Next, for a controlled reduction of $[\text{Ag}(\text{NH}_3)_2]^+$ complexes to Ag and growth of remaining Ag seeds to AgNPs on APSiO_2 , 10 mL of formaldehyde dissolved in 1 L of DW was added to the reactor slowly over 3 h through 3 openings using 3

dropping funnels while stirring. Additionally, 20 mL of formaldehyde dissolved in 200 mL of DW was added for 2 h. After further stirring for 1.5 h, the stirrer and chiller were set to the off position and the solution was left overnight without agitation. The solution was centrifuged, and the solid was washed with a 0.01% formaldehyde solution using centrifugation. Finally, the solid (51 g), which is the upper limit of yield with the reactor, was dispersed in DW to make 1 L of AgNP@SiO₂ solution.

Preparation of air filter samples coated with AgNP@SiO₂

The experimental setup for air filter coating is shown in Fig. S2. Briefly, clean air flowing at 2 L/min entered into the Collision-type atomizer, which contained a 1.3% AgNP@SiO₂ solution. The nanoparticles were aerosolized, and passed through a diffusion dryer for water removal. Finally, the generated particles were transported to coat the medium filters (Fabriano®, 4 × 4 cm²). The size distributions of the nanoparticles upstream and downstream from the filter samples were measured using a scanning mobility particle sizer (SMPS, 3936N22 Custom, TSI Inc., St. Paul, MN, USA). The SMPS system consisted of a classifier controller (3080, TSI Inc., USA), a differential mobility analyzer (DMA, 3081, TSI Inc., USA), a condensation particle counter (CPC, 3022A, TSI Inc., USA), and an aerosol charge neutralizer (Soft X-ray charger 4530, HCT Co., Ltd., Korea) and was operated at a sampling air flow rate of 300 cm³/min.

The average size of the aerosols was determined to be ~430 nm by SMPS. The particle concentrations upstream and downstream from the filter samples were 1.78 × 10⁵ particles (#)/cm³ and 1.75 × 10⁴ #/cm³, respectively. The coating areal density (ρ_{areal}) in #/cm² was calculated using Equation (1) for each coating time t :

$$\rho_{areal} [\#/cm^2] = \frac{(C^{up} - C^{down})[\#/cm^3] Q[cm^3/min] t[min]}{A[cm^2]} \quad (1)$$

where Q is the carrier gas flow rate, A is the effective cross-sectional area of the filter sample, and C is the total mass concentration of the nanoparticles. The superscripts “up” and “down” refer to the upstream and downstream locations of the filter sample, respectively. Table 1 summarizes the various coating areal densities for different coating times. The coating areal density increased linearly with the coating time.

Table 1. Summary of various coating areal densities for different coating times

Coating time t (min)	Particle concentration (#/cm ³)		Volume flow rate Q (cm ³ /min)	Effective area A (cm ²)	Coating areal density ρ_{areal} (#/cm ²)
	C^{up}	C^{down}			
1					2×10^7
3	1.78	1.75	2000	16	6×10^7
5	$\times 10^5$	$\times 10^4$			1×10^8
10					2×10^8

Preparation of bacterial solution

Two types of bacteria were selected for antibacterial tests: *Escherichia coli* (ATCC 11775) as a Gram-negative bacterium, and *Staphylococcus epidermidis* (ATCC 14990) as a Gram-positive bacterium. Both bacteria were prepared by liquid

culture, in which the desired bacteria were suspended in BD[®] Difco[™] Nutrient Broth. This liquid broth consists of approximately 3 g of beef extract and 5 g of peptone per L. After inoculation, the bacteria were grown in the liquid broth overnight in a shaking incubator (DSS 6001, Dasol MI-Tech, Korea) at 37 °C. The bacterial media were then diluted with nutrient broth so that the number of bacterial cells in the solutions was approximately 1 × 10⁶ colony forming units (CFU)/mL.

Antibacterial test

The CCM was applied to count bacterial colony numbers as follows. More specifically, 1 mL of the bacterial culture solution was added to 9 mL of DW. A filter sample, which was cut into a 1 cm diameter circular shape, was then placed into the solution and incubated with shaking at 37 °C for 24 h. The incubated solution was serially diluted with DW to obtain a countable number of colonies, and 100 μ L of each diluted solution was spread onto the surface of 87 mm × 15 mm petri dishes containing 15 mL of nutrient agar. The plates were then cultured in an incubator at 37 °C for 24 h, after which the number of CFUs per sample was determined by counting. The results of each experimental method were averaged from a dozen replications. Antibacterial efficiency (η_{CCM}) was calculated by the following Equation (2):

$$\eta_{CCM} = \left(1 - \frac{CFU}{CFU_0}\right) \times 100\% \quad (2)$$

where the subscript ‘0’ indicates the control case (*i.e.*, bacterial concentration when exposed to a filter sample without AgNP@SiO₂).

Interaction of bacteria with AgNP@SiO₂-coated air filters in air

Fifty mL of bacterial solution, which was obtained after shaking incubation for 4 h, was centrifuged and the pellet was dissolved in 50 mL of DW. The centrifuging process was performed two more times with the same operating conditions. Then, the solution was diluted with DW to an optical density (OD) of 0.1 as measured using a photospectrometer (Libra S12, Biochrom Ltd., UK) at a wavelength of 600 nm. Fifty mL of the solution was aerosolized and deposited onto the coated air filter sample that was prepared with a coating areal density of 2 × 10⁸ #/cm² using the experimental setup shown in Fig. S2. These samples were subsequently analyzed by SEM.

Interaction of bacteria with AgNP@SiO₂ in aqueous solution

Ten mL of bacterial solution (OD = 0.1) was prepared according to the same process described for bacterial deposition onto the coated air filter. Five mL of the bacterial solution was mixed with 5 mL of 0.01% AgNP@SiO₂ solution and the mixture was incubated under shaking at 30 °C for 0, 10, and 30 min. Ten μ L of incubated solution was dropped onto a silicon wafer for analysis by SEM.

Results and discussion

To serve as support materials for the hybrid structure, a large amount of silica spheres were prepared by modifying the Stöber process.²⁷ Briefly, silica spheres were grown successively until they reached ~400 nm and then functionalized with AP

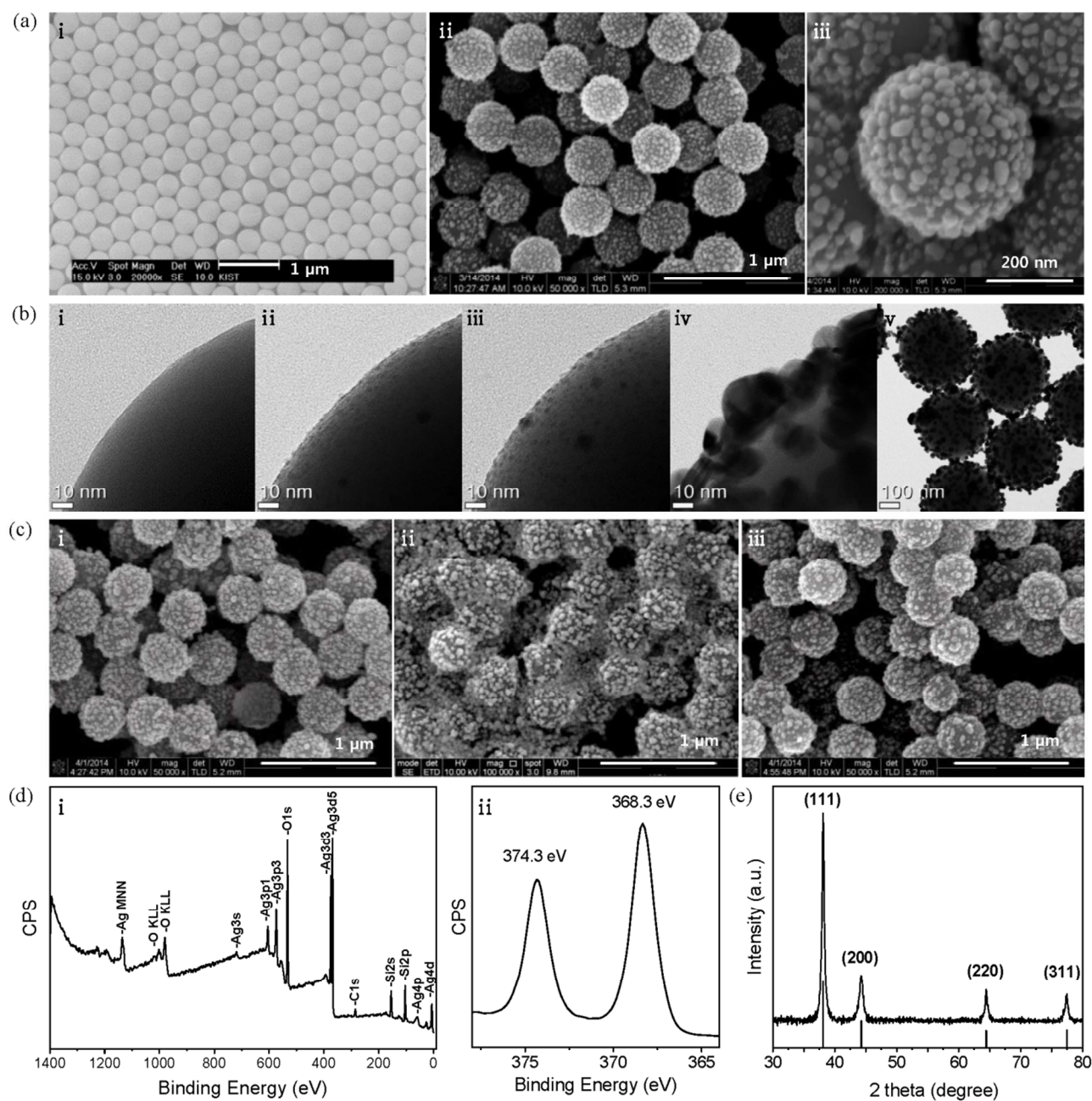
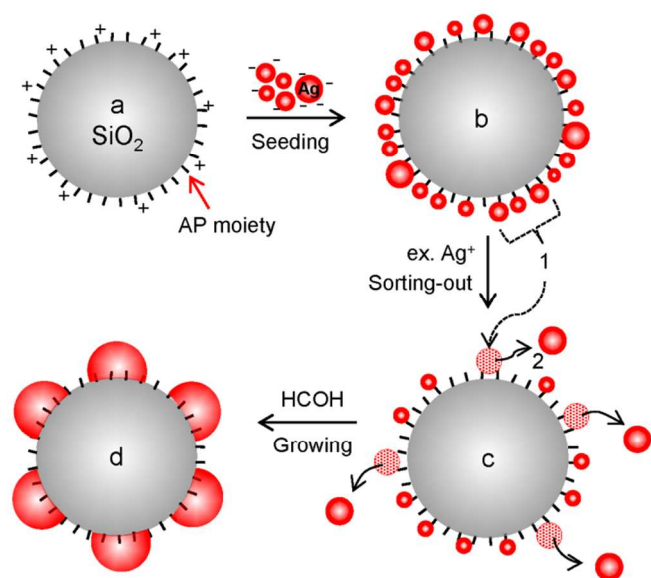


Fig. 1 (a) SEM images of (i) SiO₂ particles, (ii) AgNP@SiO₂ particles, and (iii) a single AgNP@SiO₂ particle, (b) TEM images of part of a hybrid structure for (i) initial AP-SiO₂, (ii) after Ag seeding, (iii) after sorting-out, (iv) after growing, and of (v) AgNP@SiO₂ particles, (c) SEM images of (i) 1.3% AgNP@SiO₂ solution, after 8 months, (ii) × 10 dilution, after 1 month, and (iii) × 10 dilution in 5 #% SiO₂/Fe₃O₄ solution, after 1 month, (d) XPS (i) survey scan spectrum and (ii) the corresponding specific spectrum of Ag element, and (e) XRD pattern of AgNP@SiO₂ particles (lines: JCPDS File No. 04-0783).

moieties in a one-pot synthesis. This process yielded 424 g of AP-functionalized silica spheres (AP-SiO₂) with diameter of 406 ± 17 nm (average \pm standard deviation from TEM image in Fig. S3). Their SEM image is shown in Fig. 1a i. For an application of AgNP@SiO₂ hybrid materials, we have chosen an air filter with a coating system using an atomizer. Thus, an average diameter of ~ 400 nm was chosen to avoid the most penetrated particle size range (100–300 nm),²⁸ where the aerosol coating efficiency is the lowest, and to avoid aggregation, which

frequently occurs with sizes smaller than ~ 100 nm. Fig. 1a ii and iii show SEM images of highly monodisperse AgNP@SiO₂ hybrid particles that were fabricated on the 51 g scale. Monodisperse coating material provides many advantages because the coating system becomes practically simple and economical due to fewer variable factors and the performance of the coated products becomes more reliable. The bright spots designating decorated AgNPs show a relatively



Scheme 1. Illustration for the fabrication process of an AgNP@SiO₂ hybrid particle.

homogeneous distribution with some distance between the particles on AP-SiO_2 . The undecorated part of AP-SiO_2 hybrid exposes AP moieties, which are essential for the water-dispersive property of the AgNP@SiO₂ hybrid colloids.

Overall process for the hybridization reaction is illustrated in Scheme 1. Fig. 1b i –iv show TEM images of a magnified part of each hybrid particle through the fabrication process. Corresponding TEM images of whole hybrid particles are included in Fig. S4. Fig. 1b i shows the smooth surface of a part of AP-SiO_2 and corresponds to Scheme 1a. Figure 1b ii shows densely self-assembled Ag seeds on AP-SiO_2 ($\text{Ag}_{\text{seed}}@SiO_2$) and corresponds to Scheme 1b. The reaction for self-assembly of Ag seeds on AP-SiO_2 was delicate and different from that of Ag seeds on $\text{AP-SiO}_2/\text{Fe}_3\text{O}_4$ ²⁰ or from that of Au seeds on AP-SiO_2 .²⁹ The labile property of a bond between amine and Ag seed is considered not to allow a seeding by coordinative bonding whereas it works nicely in the case of Au seeds.^{29–31} Thus, an electrostatic interaction was used to self-assemble negatively charged THPC-protected Ag seeds on a positively charged AP-SiO_2 at pH~4. In the case of Ag seeding on $\text{AP-SiO}_2/\text{Fe}_3\text{O}_4$, the Fe_3O_4 core seems to play a role as a stabilizer for the seeded hybrid structure of $\text{Ag}_{\text{seed}}@SiO_2/\text{Fe}_3\text{O}_4$ thanks to its reducing property³² of Ag^+ to Ag. However, large-scale fabrication with monodisperse size distribution is limited in the case of AgNP@SiO₂/Fe₃O₄ hybrid particles, because the silica-encapsulation reaction of Fe₃O₄ core requires a highly diluted condition to avoid aggregation and the resultant product SiO₂/Fe₃O₄ exhibits a range (0.5–0.7 μm) of size distribution.²⁰ For a successful seeding on AP-SiO_2 , a large portion of well-controlled Ag seeds in the 1–2 nm range was required. Those seeds were obtained by optimizing the molar ratio of THPC:Ag to 1:1 and by adding Ag^+ into a THPC solution rather than the *vice versa*. The AP-SiO_2 solution (pH~4) was poured into the alkaline THPC-protected Ag seed solution and gently swirled intermittently for seeding. When the centrifuged and re-dispersed $\text{Ag}_{\text{seed}}@SiO_2$ solution was poured into an Ag^+ solution containing NH₄OH and stirred, only the relatively larger seeds were displaced from the amine moieties and coalesced together (1) as shown in Fig. 1biii and Scheme 1c. The coalesced particles departed (2) from the silica particle due

to their larger inertia during stirring and at the end of the reaction, were removed by centrifugation. The stirring time of $\text{Ag}_{\text{seed}}@SiO_2$ with the Ag^+ solution containing NH₄OH was critical and was adjusted empirically. This kind of sorting-out step guaranteed some distance between the relatively small remaining seeds. This distance was necessary for the seeds to grow into the nanoparticles shown in the Fig. 1biv and Scheme 1d. During the early stage of the growth step, the remaining Ag seeds are likely to grow in all directions. During the later stage, the seeds grow upwards and sideways because there is not much space downward. Through the growth step, AP moieties are expected to be embedded in AgNPs, similar to the case of AgNPs grown from the Au seeds.²⁹ Thus, the AgNPs on the AP-SiO_2 sphere exhibit a hemisphere-like shape, which is a key for the fixation of the AgNPs on AP-SiO_2 spheres. Without the sorting-out step, the densely self-assembled Ag seeds are likely to grow to a smooth and complete shell on AP-SiO_2 .^{29,33} In the case of using Au seeds, instead of Ag seeds, growth of AgNPs from Au seeds is limited up to ~15 nm because the Au seeds pass through a different reaction pathway²⁹ from Ag seeds and the resultant hybrid particles show much lower antimicrobial effect than their corresponding hybrid particles with ~30 nm AgNPs.²⁰ The TEM image of AgNP@SiO₂ particles exhibits gray and black areas, which correspond to silica and AgNPs, respectively.

Fig. 1c shows the stability of the hybrid structure of AgNP@SiO₂ colloids with varying time and concentration in aqueous solution. The initial morphology of a 1.3% AgNP@SiO₂ solution was preserved after 8 months (i). In the case of a 5% solution, the initial morphology was preserved even after 1 year (data not shown). Therefore, the hybrid structure of AgNP@SiO₂ colloids in solution seems to be stable for use as an air filter coating, considering that the concentration we applied in the atomizer for air filter coating was 1.3% and a higher concentration would lead to higher throughput in the coating process. However, the 10-fold diluted hybrid colloids (0.13%) lost their integral morphology after only 1 month (ii). This morphological change was likely caused by oxidation and dissolution of AgNPs in the diluted aerobic solution. Interestingly, when SiO₂/Fe₃O₄ particles were added at 5% by particle number, the morphology was preserved (iii). The preservation of the hybrid structure of AgNP@SiO₂ colloids in iii can be attributed to the sacrificial oxidation of Fe²⁺ to Fe³⁺ in the Fe₃O₄ core prior to oxidation of AgNPs because the standard reduction potentials of Ag^+ to Ag and Fe³⁺ to Fe²⁺ are 0.80 V and 0.77 V, respectively.³⁴ Fig. 1d shows the XPS result of an AgNP@SiO₂ sample. The carbon 1s line was used as a reference for the binding energy scale (284.6 eV). Every line position in i is similar to those of AgNP@SiO₂/Fe₃O₄²⁰ as expected, because the magnetite core is located deep at the center of the hybrid sphere with a silica shell thickness of ~0.1 μm. Interestingly, however, the line positions of Ag 3d_{5/2} and 3d_{3/2} in the high resolution spectrum (ii) appear at 368.3 and 374.3 eV, which are 0.5 eV higher than those in AgNP@SiO₂/Fe₃O₄. This result indicates that partial oxidation of the AgNPs proceeded further on SiO₂ than on SiO₂/Fe₃O₄. Fortunately, it has been reported that partially oxidized AgNPs still exhibit antibacterial activity,^{13,14} and it will be shown later. The XRD pattern of AgNP@SiO₂ (Fig. 1e) exhibits only the face centered cubic crystalline phase of Ag metal (JCPDS File No. 04-0783) because silica is amorphous. The UV–Vis absorption spectrum of AgNP@SiO₂ (Fig. S5) shows a typical plasmonic peak³³ of AgNPs at 410 nm as well as their associated peak at ~600 nm.

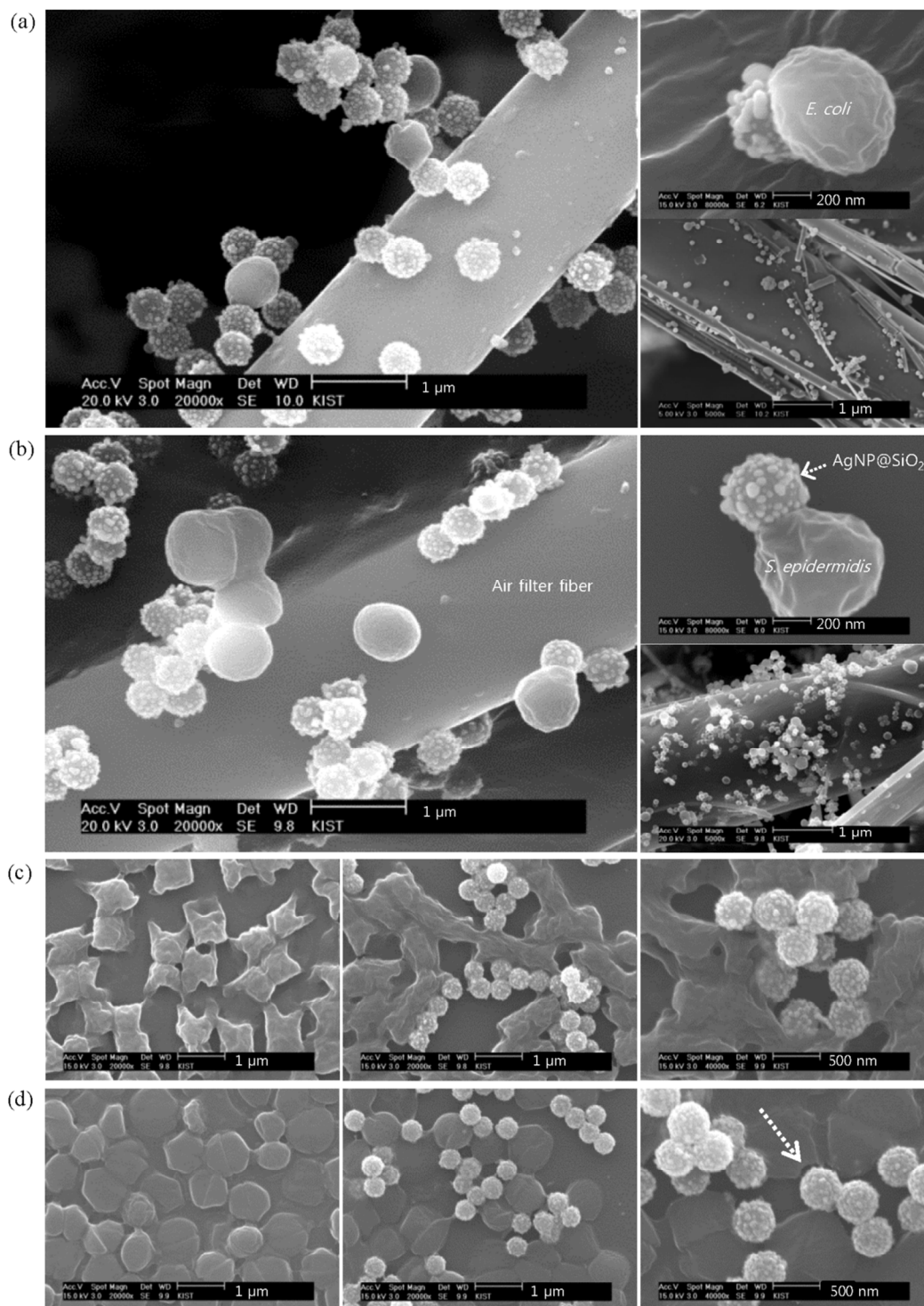


Fig. 2 SEM images of (a) *E. coli* and (b) *S. epidermidis* deposited on the AgNP@SiO₂-coated air filter at different magnifications and (c) *E. coli* and (d) *S. epidermidis* incubated in AgNP@SiO₂ solution for 0, 10, and 30 min (left, middle, and right, respectively).

As an example for application, AgNP@SiO₂ aerosols were generated from AgNP@SiO₂ colloidal solution *via* a Collision atomizer and coated on the air filter samples using the

experimental setup in Fig. S2. The coated filter samples with varying coating times and particle concentrations are summarized in Table 1. First, we wanted to examine whether

the coated AgNP@SiO₂ particles exhibit antibacterial activity on air filtration. For this purpose, the selected bacterial aerosols carried by clean air at 2 L/min were deposited on the AgNP@SiO₂-coated filter samples with coating areal density of 2×10^8 #/cm². SEM images of these samples with different magnifications are displayed in Fig. 2a and b for *E. coli* and *S. epidermidis*, respectively. The coated AgNP@SiO₂ aerosols show a relatively homogeneous distribution on the filter. Relatively larger ellipsoids (~0.6 μm) in a and spheres (~0.8 μm) in b represent *E. coli* and *S. epidermidis*, respectively and it agrees with the published data.^{35,36} Strikingly, both bacteria are trapped by AgNP@SiO₂ hybrid particles coated on the filter fiber and a single AgNP@SiO₂ hybrid particle is enough to trap each bacterium. Furthermore, the trapped bacteria do not seem to be viable, possibly because the trap is so strong that the bacteria cannot escape without rupturing their cellular membrane or cell wall. Plentiful AgNPs protruded on a silica support are considered to play a key role as many teeth to bite bacteria and led to cell death by chemisorption of Mg²⁺ or Ca²⁺ ions from bacterial surface as will be discussed later. To the authors' knowledge, this is the first explicit evidence for a coated material showing the prompt antibacterial activity on air filtration.

It would be useful to know whether the interaction between AgNP@SiO₂ hybrid particles and bacteria in air is the same as in water. Thus, the temporal morphology of the bacteria was investigated while incubating their aqueous mixtures with AgNP@SiO₂ hybrid colloids. SEM images from this experiment are displayed in Fig. 2c and d, and Fig. S6. In the case of *E. coli*, their morphology (ellipsoid, a) trapped on the filter looks different from that (c i) dropped on the silicon wafer. The morphology of *E. coli* on the filter has been preserved during Pd/Pt sputtering for SEM sample preparation because they were deposited on the filter fiber in three-dimensional space after passing through a diffusion dryer. On the other hand, the dropped and dried *E. coli* on the silicon wafer with two-dimensional surface exhibits rich surface morphology as reported,³⁷ due to a chemical etching by plasma during Pd/Pt sputtering. Plasma is known to etch away the outer membrane according to a treated time and cause shrinkage of *E. coli* (ATCC 11775).³⁷ The *E. coli* bacteria seem to be disrupted promptly upon contact with AgNP@SiO₂ colloids. No pristine bacteria were present, even at 10 min. In the case of *S. epidermidis*, most AgNP@SiO₂ colloids seem to bite bacteria promptly at their first contact (10 min image). In contrast to the morphology (sphere) of bacteria trapped on the coated air filter,

the morphology of *S. epidermidis* on the silicon wafer exhibited additionally a flattened disk shape, which seems to be caused by the Pd/Pt sputtering on the wafer for SEM sample preparation.³⁷ Bitten traces are indicated as an arrow in Fig. 2d and Fig. S6b. The bitten traces appear to be separated from the AgNPs on the silica sphere by sputtering impact. Therefore, we deduced that the bacteria trapped on AgNP@SiO₂ hybrid particles coated on the air filter will lead cell disruption meaning cell death and many AgNPs decorated on the silica sphere play that role promptly and synergistically. That is, a single AgNP with partially naked surface can make a pit on the Gram-negative bacterial membrane,⁹ whereas a single AgNP@SiO₂ hybrid particle can disrupt a bacterial membrane or cell wall upon contact. Cell viability test which will be shown later with Fig. 3b and c can support our deduction. This type of prompt antibacterial effect from AgNP@SiO₂ hybrid particles may be particularly promising for treatment of antibiotic-resistant microorganisms such as super-bacteria. The prompt and fatal antibacterial activity of AgNP@SiO₂ hybrid particles is attributed to the naked AgNPs and their teeth-like synergistic effect in a three-dimensional structure. Like the case of AgNP@SiO₂/Fe₃O₄ hybrid particles,²⁰ the naked AgNPs chemically adsorb Mg²⁺ or Ca²⁺ ions from the Gram-negative bacterial membrane that contains tightly packed lipopolysaccharides (LPS). Within the membrane, metal ions such as Mg²⁺ and Ca²⁺ play an essential role in preserving the structure by strengthening the LPS interactions.³⁸ The same mechanism is also likely responsible for efficacy against the Gram-positive bacteria. In the case of Gram-positive bacteria, the thick peptidoglycan layer of the cell wall is known to be resistant to the penetration of Ag⁺ ions.⁸ However, the peptidoglycan layer is also strengthened by metal ions, as Mg²⁺ and Ca²⁺ ions are known to form bridges across phosphate groups in adjacent teichoic acid chains in the Gram-positive bacterial cell wall.³⁹ Thus, the naked AgNPs decorated on the silica sphere seem to pressurize the spots where the metal ions are bridged in the thick bacterial cell wall and chemically adsorb Mg²⁺ or Ca²⁺ ions, as observed on the right top side of Fig. 2b. Due to the thick bacterial cell wall, the bacteria stay attached to the AgNP@SiO₂ hybrid particles until they are disrupted by external force, as indicated by the arrow in Fig. 2d and Fig. S6b. From these images and viability test in Fig. 3b and c, the trapped bacteria are assumed to be dead. Therefore, in both Gram-negative and Gram-positive bacteria, the bacterial trapping by AgNP@SiO₂ hybrid particle implicates cell death.

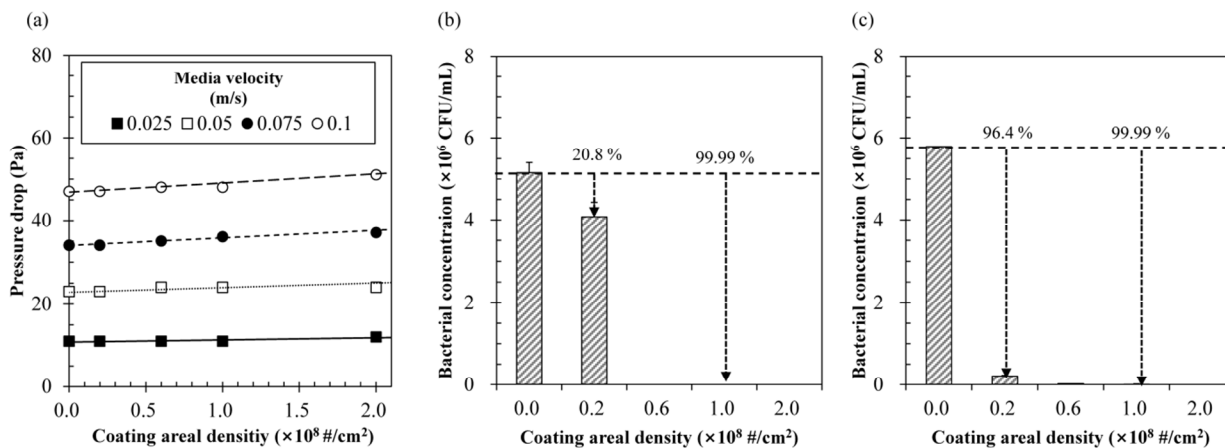


Fig. 3 (a) Pressure drop and antibacterial efficacy of AgNP@SiO₂-coated air filter samples for (b) *E. coli* and (c) *S. epidermidis*.

The air filter samples summarized in Table 1 all showed a coating efficiency of AgNP@SiO₂ particles greater than 90%. No meaningful detachment of AgNP@SiO₂ particles were observed from the coated air filter samples, even when a clean air flow of 10 L/min was forced onto them. In Fig. 3a, the pressure drops caused by coating increased linearly with the increasing coating areal density at constant media velocity but are acceptable because the variation was generally within 5%. At a media velocity of 0.025 m/s, the filtration efficiencies of bioaerosols were 91 and 95% for the air filter samples with the coating areal densities of 6×10^7 and 2×10^8 #/cm², respectively. Although the CCM or the DDM does not exactly reflect antibacterial activity in air, we performed cell viability test using the CCM because there is no better alternative in the present case. In Fig. 3b and c, the antibacterial efficacies determined by the CCM were high (*i.e.*, > 99.99%) against both *E. coli* and *S. epidermidis* in solutions containing the filter samples with a coating areal density $\geq 1 \times 10^8$ #/cm².

Conclusions

In conclusion, we have presented large-scale (51 g) fabrication of highly monodisperse AgNP@SiO₂ hybrid particles and have shown their prompt and synergistic antibacterial activity against both Gram-negative and Gram-positive bacteria on air filtration. The AgNP@SiO₂ hybrid particles showed antibacterial activity promptly and synergistically by the naked AgNPs on the silica sphere upon contacting bacteria. Further study on the antimicrobial effects using the AgNP@SiO₂-coated air filter and viruses showed promising results and will be published elsewhere. The hybrid particle AgNP@SiO₂ and the devices or appliances coated with the particles are expected to be useful for future green environment applications.

Acknowledgements

This research was supported by the Future-based Technology Development Program (Green Nano Technology Development Program) through the National Research Foundation of Korea funded by the Ministry of Science, ICT & Future Planning (Grant No. 2013-069323 and 2013-069325) and the KIST institutional program (Project No. 2E24860).

Notes and references

^a Molecular Recognition Research Center, Korea Institute of Science and Technology, P. O. Box 131, Cheongryang, Seoul 130-650, Korea

^b School of Mechanical Engineering, Yonsei University, Seoul 120-749, Korea

^c Korea University of Science and Technology

† Electronic Supplementary Information (ESI) available: A photograph of tailor-made 50 L reactor, experimental setup for fabrication of antibacterial air filters, TEM and SEM images, UV-Vis absorption spectrum. See DOI: 10.1039/b000000x/

- 1 R. Maus, A. Goppelsröder, H. Umhauer, *Atmos. Environ.*, 2001, **35**, 105.
- 2 M. C. Verdenelli, C. Cecchini, C. Orpianesi, G. M. Dadea, A. Cresci, *J. Appl. Microbiol.*, 2003, **94**, 9.

- 3 C. Cecchini, M. C. Verdenelli, C. Orpianesi, G. M. Dadea, A. Cresci, *J. Appl. Microbiol.*, 2004, **97**, 371.
- 4 K. Y. Yoon, J. H. Byeon, C. W. Park., J. Hwang, *Environ. Sci. Technol.*, 2008, **42**, 1251.
- 5 E. Miałkiewica-Peska, M. Łebkowska, *Fibres Text. East. Eur.*, 2011, **19**, 73.
- 6 S. J. Park, Y. S. Jang, *J. Colloid Interface Sci.*, 2003, **261**, 238.
- 7 J. H. Byeon, K. Y. Yoon, J. H. Park, J. Hwang, *Carbon*, 2007, **45**, 2313.
- 8 Q. L. Feng, J. Wu, G. Q. Chen, F. Z. Cui, T. N. Kim, J. O. Kim, *J. Biomed. Mater.*, 2000, **52**, 662.
- 9 I. Sondi, B. Salopek-Sondi, *J. Colloid Interface Sci.*, 2004, **275**, 177.
- 10 M. Rai, A. Yadav, A. Gade, *Biotechnol. Adv.*, 2009, **27**, 76.
- 11 C. Marambio-Jones, E. M. V. Hoek, *J. Nanopart. Res.*, 2010, **12**, 1531.
- 12 S. Eckhardt, P. S. Brunetto, J. Gagnon, M. Priebe, B. Giese, K. M. Fromm, *Chem. Rev.*, 2013, **113**, 4708.
- 13 A. Kumar, P. K. Vemula, P. M. Ajayan, G. John, *Nature Mater.*, 2008, **7**, 236.
- 14 C.-N. Lok, C.-M. Ho, R. Chen, Q.-Y. He, W.-Y. Yu, H. Sun, P. K.-H. Tam, J.-F. Chiu, C.-M. Che, *J. Biol. Inorg. Chem.*, 2007, **12**, 527.
- 15 O. Choi, K. K. Deng, N.-J. Kim, L. Jr. Ross, R. Y. Surampalli, Z. Hu, *Water Res.*, 2008, **42**, 3066.
- 16 Z. Xiu, Q. Zhang, H. L. Puppala, V. L. Colvin, P. J. J. Alvarez, *Nano Lett.*, 2012, **12**, 4271.
- 17 W.-R. Li, X.-B. Xie, Q.-S. Shi, H.-Y. Zeng, Y.-S. OU-Yang, Y.-B. Chen, *Appl. Microbiol. Biotechnol.*, 2010, **85**, 1115.
- 18 G. A. Sotiriou, S. E. Pratsinis, *Environ. Sci. Technol.*, 2010, **44**, 5649.
- 19 A. Panáček, L. Kvítek, R. Prucek, M. Kolář, R. Večeřová, N. Pizúrová, V. K. Sharma, T. Nevěčná, R. Zbořil, *J. Phys. Chem. B*, 2006, **110**, 16248.
- 20 H. H. Park, S. Park, G. Ko, K. Woo, *J. Mater. Chem. B*, 2013, **1**, 2701.
- 21 L. Zhang, Q. Luo, F. Zhang, D.-M. Zhang, Y.-S. Wang, Y.-L. Sun, W.-F. Dong, J.-Q. Liu, Q.-S. Huo and H.-B. Sun, *J. Mater. Chem.*, 2012, **22**, 23741.
- 22 J. H. Byeon, B. J. Ko, J. Hwang, *J. Phys. Chem. C*, 2008, **112**, 3627.
- 23 K.-Y. Yoon, J. H. Byeon, J.-H. Park, J. H. Ji, G. N. Bae, J. Hwang, *Environ. Eng. Sci.*, 2008, **25**, 289.
- 24 B. U. Lee, S. H. Yun, J.-H. Ji, G.-N. Bae, *J. Microbiol. Biotechnol.*, 2008, **18**, 176.
- 25 Y. H. Joe, W. Ju, J. H. Park, Y. H. Yoon, J. Hwang, *Aerosol Air Qual. Res.*, 2013, **13**, 1009.
- 26 J. H. Jung, G. B. Hwang, J. E. Lee, G. N. Bae, *Langmuir*, 2011, **27**, 10256.
- 27 W. Stöber, A. Fink, E. Bohn, *J. Colloid Interface Sci.*, 1968, **26**, 62.
- 28 Y. Qian, K. Willeke, S. A. Grinshpun, J. Donnelly, C. C. Coffey, *Am. Ind. Hyg. Assoc. J.*, 1998, **59**, 128.
- 29 H. H. Park, K. Woo, J.-P. Ahn, *Sci. Rep.* **3**, 1497; DOI: 10.1038/srep01497 (2013).
- 30 A. Kumar, H. Joshi, R. Pasricha, A. B. Mandale, M. Sastry, *J. Colloid Interface Sci.*, 2003, **264**, 396.
- 31 D. V. Leff, L. Brandt, J. R. Heath, *Langmuir*, 1996, **12**, 4723.
- 32 J. Liu, Z. Zhao, H. Feng, F. Cui, *J. Mater. Chem.*, 2012, **22**, 13891.
- 33 J. B. Jackson, N. J. Halas, *J. Phys. Chem. B*, 2001, **105**, 2743.

Journal Name

- 34 A. J. Bard, L. R. Faulkner, *Electrochemical Methods: Fundamentals and Applications*; John Wiley & Sons, Inc.: New York, 2001, p 808.
- 35 S. Joshi, G. S. Bisht, D. S. Rawat, A. Kumar, R. Kumar, S. Maiti, S. Pasha, *Biochim. Biophys. Acta*, 2010, **1798**, 1864.
- 36 W. Ziebuhr, C. Heilmann, F. Götz, P. Meyer, K. Wilms, E. Straube, J. Hacker, *Infect. Immun.*, 1997, **65**, 890.
- 37 D. Vujošević, M. Mozetič, U. Cvelbar, N. Krstulović, S. Milošević, *J. Appl. Phys.*, 2007, **101**, 103305.
- 38 N. A. Amro, L. P. Kotra, K. Wadu-Mesthrige, A. Bulychev, S. Mobashery, G.-y. Liu, *Langmuir*, 2000, **16**, 2789.
- 39 I. Sadovskaya, E. Vinogradov, J. Li, S. Jabbouri, *Carbohydr. Res.*, 2004, **339**, 1467.

Graphical abstract

Silver nanoparticle-decorated silica hybrid particles (AgNP@SiO₂) bite away bacteria promptly and synergistically upon contact by air filtration.

Contents figure